Journal of Computers Vol. 30 No. 1, 2019, pp. 183-196
doi:10.3966/199115992019023001018

Non-contact Optical Image Analysis and Measurement of Heartbeat Method

Hsien-Wei Tseng[1*], Yang-Han Lee[1,2], Chien-Da Huang[2], Yu-De Liao[2], Ting-Wei Lin[2], Ting-Cheng Chang[3]

[1] School of Information Engineering, Longyan University, Longyan, Fujian, China
hsienwei.tseng@gmail.com

[2] Department of Electrical and Computer Engineering, Tamkang University, Taiwan , R.O.C
yhleepp@gmail.com, darvan@benegear.com, lflf3322@gmail.com, twlin@gms.tku.edu.tw

[3] Department of Computer and Information Engineering, Ningde Normal University, Fujian, China
18250922163@163.com

Received 30 September 2017; Revised 29 October 2017; Accepted 10 January 2018

Abstract. Noncontact detection refers to using external energy to detect human physiological information changes without contacting the human body. Because noncontact detection devices are exceedingly expensive and unavailable, using them on average families or for personal use is inappropriate. This study designed an image-based noncontact heartbeat measurement method for determining heartbeats by using varying light absorption on the human face. By performing image processing and independent components analysis, hidden information in the images were identified and concentrated before conducting frequency domain transform and heartbeat estimation processes, thereby achieving noncontact automatic measurement.

Keywords: Electrocardiography (ECG), Fast Fourier Transform (FFT), image processing, non-contact, Independent Components Analysis (ICA)

1 Introduction

Heartbeat information is a crucial indicator in the clinical detection of life parameters. Current mainstream methods used for detecting heartbeats are contact detection technologies, such as electrocardiography (ECG) [1] and photoplethysmography (PPG) [2]. Thus far, ECG has been a suitable indicator for evaluating physical health status. The major advantage of the contact detection methods is noninvasive measurements and complete waveforms, which can provide clinical references for physicians. However, measuring using ECG requires applying electrically conductive gel as a medium to attach conductive elec-trode pads onto the chest of the subject, rendering a low level of convenience for the user. The PPG refers to the signal of blood pressure changes sensed using optical sensing. The measurement method involves emitting lights on a selected skin area. The light enters the skin and is absorbed by blood, generating con-tinual variations. The graph depicted according to the continual variation of light is the PPG. The ad-vantage of PPG is that little electrical noise is produced. Although PPG requires measurement devices to be worn, it is more convenient for users, compared with ECG.

Noncontact detection [3-6] refers to using external energy to detect the physiological information changes in the human body without contacting the human body. Noncontact life detection technologies include infrared, laser, microwave, and acoustic wave sensing technologies. As a noncontact physiological information detection method, microwave sensing technology is a radar-based noncontact life detection technology applying an electromagnetic wave as a medium for measuring physical vibration caused by human physiological activities. Electromagnetic waves emitted to the human body reflects partial physio-logical information of the human body. Based on the relationship between human-

* Corresponding Author

body micromovement and the magnitude and phase of reflection waves, crucial physiological information can be extracted. And use the method of ICA experiment to get the correct signal.

2 Independent Components Analysis

Independent components analysis (ICA) [7] is a statistical and computational technique. The main function of ICA is to determine random variables or hidden factors in signals. ICA is similar to blind source separation (BSS), which involves separating unknown independent signal sources from the collected information or signals [8-10]. For multiple observation data obtained from large sample databases, ICA defines a generative model, which involves a hypothesis that states that the observed data are a linear or nonlinear mixture of unknown internal variables. Moreover, not only are the internal variables unknown, but the system implementing the mixture is also unknown. If the internal variables are hypothesized as non-Gaussian distributed and mutually independent, these variables are referred to as independent components of the observation data and can be determined using ICA.

2.1 Basic Concepts

ICA is most commonly used in processing voice signals and is frequently used in the solution to the cocktail party problem [11]. As shown in Fig. 1, when three people with different timbres sing simultaneously in a space and three microphones receive the sound in different places, the independent signal sources of the three people are referred to as $(s_1(t), s_2(t), s_3(t))$, and the mixed signals received by the microphones are $(x_1(t), x_2(t), x_3(t))$. If the measured mixed signals are unknown linear combinations, the signals can be expressed as follows:

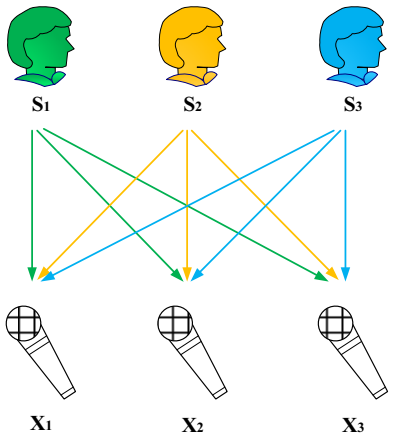

Fig. 1. Schematic cocktail party problem

$$\begin{aligned} x_1(t) &= a_{11}s_1(t) + a_{12}s_2(t) + a_{13}s_3(t) \\ x_2(t) &= a_{21}s_1(t) + a_{22}s_2(t) + a_{23}s_3(t) \\ x_3(t) &= a_{31}s_1(t) + a_{32}s_2(t) + a_{33}s_3(t) \end{aligned} \tag{1}$$

where $a_{11}, a_{12}, a_{13}, a_{22}, a_{23}, a_{31}, a_{32}, a_{33}$ are weights that the microphones receive. The parameter values are related to the distance between the microphones and the sound source. Equation (1) can be rewritten into a matrix as follows:

$$\begin{bmatrix} x_1(t) \\ x_2(t) \\ x_3(t) \end{bmatrix} = \begin{bmatrix} a_{11} & a_{12} & a_{13} \\ a_{21} & a_{22} & a_{23} \\ a_{31} & a_{32} & a_{33} \end{bmatrix} \begin{bmatrix} s_1(t) \\ s_2(t) \\ s_3(t) \end{bmatrix} \tag{2}$$

where matrix A is considered a mixing matrix and matrix S represents the sound source signals. Generally, the microphone signal values are the only available data. When matrix A is unknown,

calculating the original sound source values is difficult. However, ICA [12] can be used for analyzing and estimating the original sound sources even when matrix A is unknown.

2.2 Computational Process

To determine the original signal source, the separation matrix W and the original mixing matrix A must be similar. By performing ICA, independent components are constantly identified from mixing signal X. In addition, optimization methods are used for improving the independency between signals, thereby solving the separation matrix W and determining the estimation vector Z. Subsequently, the mixing matrix A can be solved and original signal source S determined, as shown in Fig. 2.

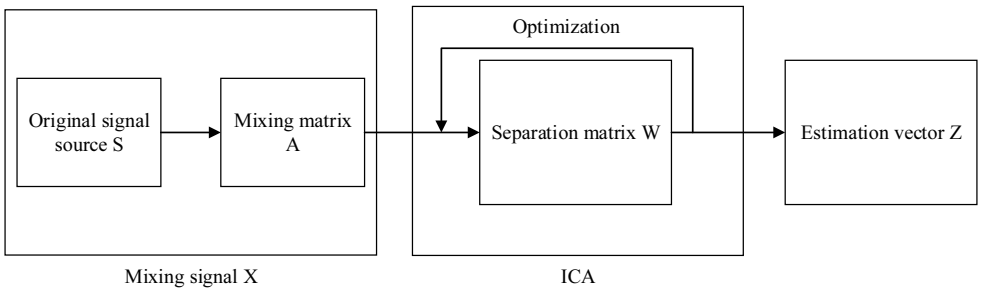

Fig. 2. Brief procedure of ICA

Definition 1.

Centering: The most fundamental and necessary preprocessing is the centering of mixing signal X by deducing the mean of the signal to enable the processed signal to reach zero mean. The signal does not change its characteristics because of this processing. The mathematical equation is expressed as follows:

$$X_C = X - E\{X\} \tag{3}$$

where X_C is the mixing signal processed by centering

Definition 2.

Whitening: Whitening refers to the use of linear transformation to transform mixing signals from correlated signals to uncorrelated signals, concentrating variables with originally high variance to the new variables. This concept primarily involves using principal component analysis (PCA) [6]. Variables with high variance are principal components of signals, whereas those with low variance are noise sources. After variables with low variance are discarded, PCA can be used to attain the function of decreasing dimensions. The definition is expressed as follows:

$$E\{X_C X_C{}^T\} = C_{x_c} \tag{4}$$

where C_{x_c} is the covariance matrix of centered mixing signal X_C. To obtain uncorrelated signals, the covariance matrix C_{x_c} undergoes eigenvalue decomposition, which is expressed as follows:

$$C_{x_c} = UDU^T \tag{5}$$

where $\boldsymbol{U}$ is the unit orthogonal matrix composed of eigenvectors, and $\boldsymbol{D}$ is the diagonal matrix composed of eigenvalues of the covariance matrix C_{x_c}.

If a whitening matrix $\boldsymbol{V}$ performs linear transformation with centered mixing signal X_C, a new whitening mixing signal $\hat{X}$ can be obtained.

$$\hat{X} = VX_c \tag{6}$$

The whitening matrix $\boldsymbol{V}$ is defined as

$$V = C_{x_c}{}^{-1/2} = UD^{-1/2U^T} \tag{7}$$

The whitened mixing signal $\hat{X}$ is substituted into the covariance matrix $C_{\hat{x}}$.

$$C_{\hat{x}} = E\{\hat{X}\hat{X}^T\} \tag{8}$$

Definition 3.

Defining objective function: According to the central limit theorem, when probability distribution of multiple non-Gaussian distributed and mutually independent random variables is summed, the result converges toward a Gaussian distribution. Thus, to determine individual independent signals, the statistical method measuring non-Gaussian distribution must be used for determining individual independent signals. Kurtosis and negentropy are most commonly used for measuring non-Gaussian distribution and quantifying and formulating such distribution.

Definition 4.

Optimization algorithm: In this study, the Fast ICA algorithm proposed by Hyvärinen was used for optimizing the objective function defined in the previous section. The independent component y to be determined is expressed as $y = w^T x$.

$$J(w^T x) \propto [E\{G(w^T x)\} - E\{G(V)\}]^2 \tag{9}$$

In the Fast ICA [7] algorithm, the constant number α_1 in Function G is generally set as 1. Fast ICA determines the maximum of $J(w^T x)$ based on fixed-point iteration. According to Karush-Kuhn-Tucker conditions, under the limitation of $E\{G(w^T x)\}^2 = \| w \|^2 = 1$, $E\{G(w^T x)\}$ has the maximum w that must satisfy the following equation:

$$E\{xg(w^T x)\} - \beta w = 0 \tag{10}$$

where g is the differential of Function G. Subsequently, Newton's method was used for solving the equation. The left side of the equation mark is represented as F, and the Jacobian matrix can be obtained:

$$JF(w) = E\{xx^T g'(w^T x)\} - \beta \boldsymbol{I} \tag{11}$$

If signal x has undergone centering and whitening processing, to simplify (11), approximation such as $E\{xx^T g'(w^T x)\} \approx -E\{xx^T\}E\{g'(w^T x)\} = E\{g'(w^T x)\}\boldsymbol{I}$ can be performed before using Newton's method. The following iteration equation is obtained:

$$w_{new} = w_{old} - \frac{[E\{xg({w_{old}}^T x)\} - \beta w_{old}]}{[E\{g'({w_{old}}^T x)\} - \beta]} \tag{12}$$

When both sides of the equation are multiplied by $\beta - E\{g'({w_{old}}^T x)\}$, (12) is rewritten as follows:

$$w_{new} = E\{xg({w_{old}}^T x)\} - E\{g'({w_{old}}^T x)\} w_{old} \tag{13}$$

If the w_{new} and w_{old} have the same direction, they are in convergence, which means that $w_{new} \cdot w_{old} \approx 1$.

In the iteration process, an initial random set of vector $\boldsymbol{w}$ is generated before calculating iterations using (13) for determining the decorrelation vector $\boldsymbol{w}$ in the separation matrix $\boldsymbol{W}$. However, the results after iteration do not guarantee the orthogonality of each vector. Thus, the decorrelation vector $\boldsymbol{w}_{n+1}$ determined after each iteration must deduct the direction of decorrelation vector $\boldsymbol{w}$ determined in previous n iterations to achieve the orthogonality between vectors. The equation is expressed as follows:

$$w_{n+1} = w_{n+1} - \sum_{j=1}^{n} ({w_{n+1}}^T w_j) w_j \tag{14}$$

where $\boldsymbol{w}_j$ is the decorrelation vector after previous iterations; j = 1,2,3,…,n, and the decorrelation vector $\boldsymbol{w}$ is normalized:

$$w_{n+1} = w_{n+1} / \sqrt{{w_{n+1}}^T w_{n+1}} \tag{15}$$

Finally, all of the determined decorrelation vectors ***w*** compose the separation matrix ***W*** for calculating the estimation vector ***Z***. The Fast ICA algorithm is expressed in a flow chart as follows in Fig. 3:

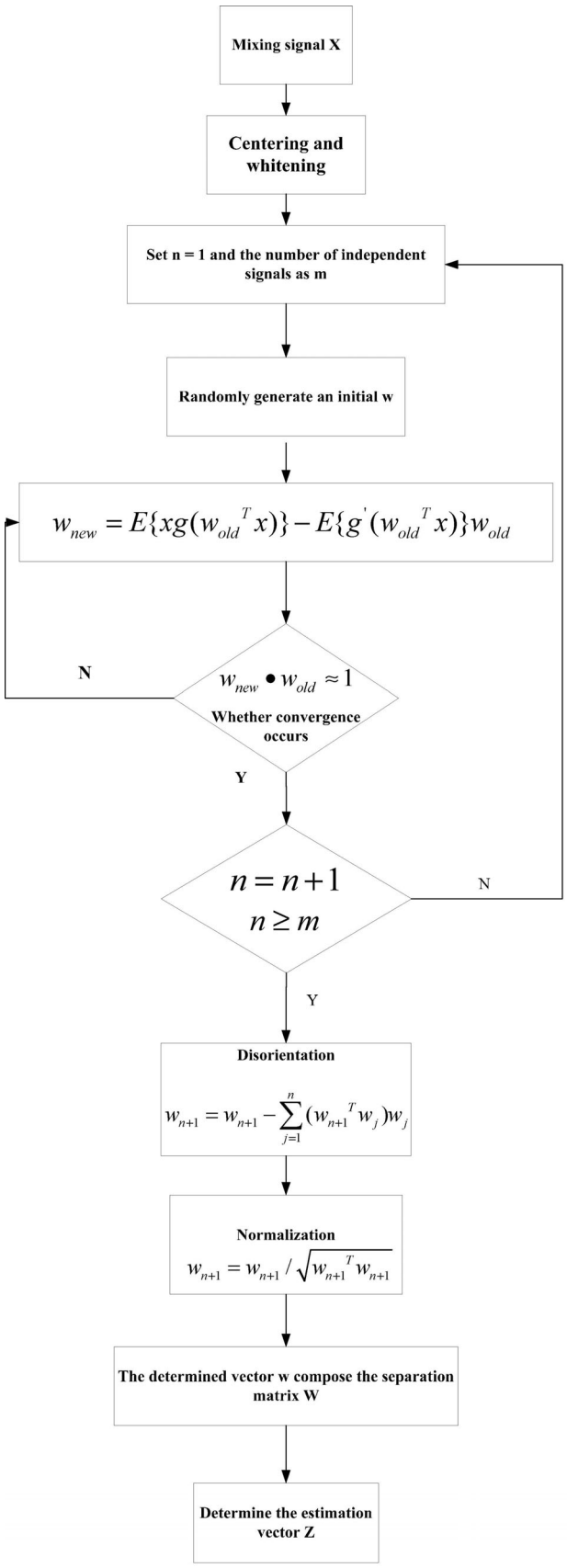

Fig. 3. Fast ICA optimization algorithm calculation process [13-14]

3 Experimental Equipment

The hardware part used in this study involved employing a video camera embedded in basic laptop computers for filming human faces. The video color was 24-bit RGB, at a 640 X 480 resolution and 30 frames per second (FPS). The software part involved using the LabVIEW platform, developed by National Instruments, combined with IMAQ Vision Function Palettes. The control group in the test used ECG devices. During experimental measurement, the participants wore the measurement device to facilitate comparison with the experimental data in this study. Fig. 3 shows the state during measurement as shown in Fig. 4.

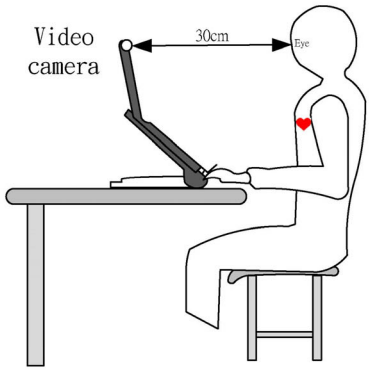

Fig. 4. Measurement state diagram [15-18]

4 Experimental Procedure

After the image was photographed, image preprocessing was conducted, including color channel separation, selection of region of interest (ROI), and calculation of color histogram means [12]. The color histogram means of the three channels measured during image preprocessing were processed using ICA. The values of the three independent components were determined. Subsequently, fast Fourier analysis was used for determining the frequency spectrum of the color histogram means in the green channel and the data of three independent components. Within a frequency range between 0.75 and 4 Hz (heartbeat: 45-240 beats per minute; BPM), the strongest intensity in the frequency spectrum and the corresponding frequencies were determined. The highest independent component value among the frequency spectra of the three independent components was selected. Multiplying the frequency of the selected independent component by 60 determined the required heartbeat value (BPM). The frequency spectrum of the color histogram of the green channel directly converted the frequency at the maximal energy into heartbeat value (BPM). Finally, the two individual heartbeat values were compared with the heartbeat values measured using ECG devices. The flow chart as shown in Fig. 5.

5 Experimental Results

This experiment was conducted in an indoor space. During the experiment, each participant wore an ECG measurement device to facilitate a comparison with the data generated in this study. The test comprised three cases: (1) Case 1 involved a test of different skin colors, (2) Case 2 involved a test before and after exercise, and (3) Case 3 involved a test of time differences.

An error rate refers to using the value measured using ECG as the standard value. The calculation equation is shown as follows:

$$\frac{Differential\ value}{ECG\ Value} \times 100(\%) \tag{16}$$

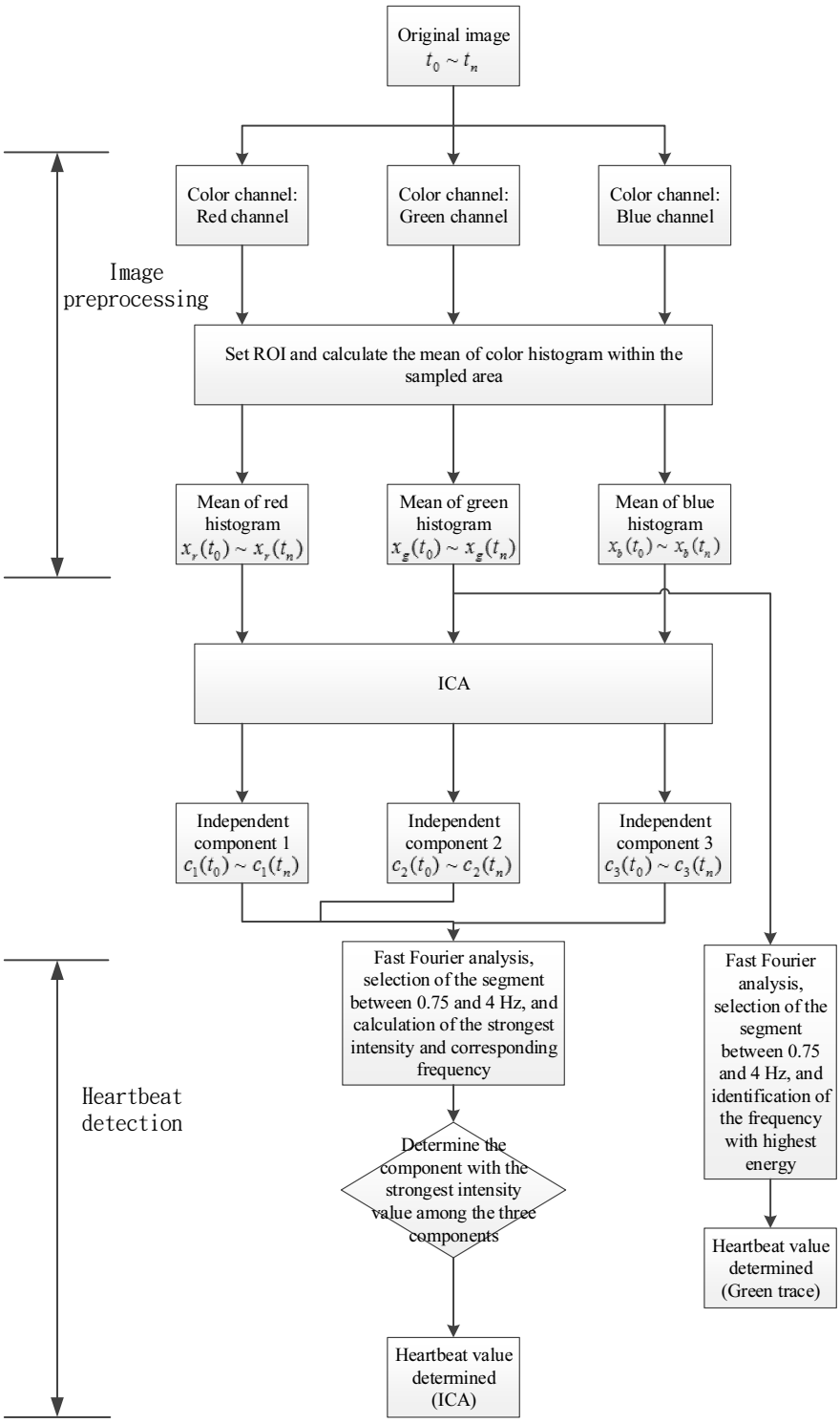

Fig. 5. Experimental procedure

5.1 Case 1: Test of Different Skin Colors

In Case 1, three participants A, B, and C with different skin colors (dark, average, and light, respectively) were recruited. The participants' physical conditions were at an average status during the test. The test time was 30 s for each iteration, and each participant was tested for 10 iterations in total. The purpose of this experiment was to ensure that the measurement values could be accurate among participants with different skin colors.

Experimental Data:

Table 1. Data of participant A (dark skin color)

Item / Iteration	Green Raw Trace (BPM)	ICA (BPM)	ECG Data (BPM)
1	62.42	62.29	63.33
2	61.66	61.79	61.73
3	61.14	60.85	63.73
4	33.76	68.15	62.36
5	61.28	61.36	62.70
6	57.86	57.87	64.26
7	54.14	54.02	56.27
8	55.23	55.23	56.50
9	60.79	60.83	61.90
10	58.18	58.20	61.03

Table 2. Data of participant B (average skin color)

Item / Iteration	Green Raw Trace (BPM)	ICA (BPM)	ECG Data (BPM)
1	65.55	60.58	62.87
2	59.33	59.20	62.53
3	60.77	62.78	65.10
4	64.75	65.05	73.07
5	50.97	67.21	68.73
6	67.39	68.06	66.35
7	66.64	66.38	67.14
8	67.09	67.33	67.42
9	66.71	72.54	73.78
10	64.51	64.95	69.67

Table 3. Data of participant C (light skin color)

Item / Iteration	Green Raw Trace (BPM)	ICA (BPM)	ECG Data (BPM)
1	44.73	64.51	62.83
2	61.07	61.16	61.93
3	60.08	60.03	61.35
4	62.01	61.78	65.46
5	63.93	61.27	60.83
6	59.70	59.64	65.90
7	70.68	70.88	70.23
8	67.73	67.85	69.12
9	68.33	68.27	69.25
10	63.14	63.52	64.31

Error Rate Comparison:

Table 4. Differential values and error rates of participant A (dark skin color)

Item / Iteration	Green Raw Trace V.S ECG Differential Value (BPM)	ICA V.S ECG Differential Value (BPM)	Green Raw Trace V.S ECG Error Rate (%)	ICA V.S ECG Error Rate (%)
1	0.91	1.04	1.44	1.65
2	0.07	0.05	0.11	0.09
3	2.59	2.88	4.07	4.52
4	28.60	5.79	45.86	9.28
5	1.42	1.34	2.27	2.14
6	6.40	6.39	9.95	9.94
7	2.13	2.25	3.78	4.00
8	1.27	1.27	2.25	2.24
9	1.11	1.07	1.79	1.73
10	2.85	2.83	4.67	4.64
Mean	4.73	2.49	7.62	4.02

Table 5. Differential values and error rates of participant B (average skin color)

Item / Iteration	Green Raw Trace V.S ECG Differential Value (BPM)	ICA V.S ECG Differential Value (BPM)	Green Raw Trace V.S ECG Error Rate (%)	ICA V.S ECG Error Rate (%)
1	2.68	2.29	4.26	3.64
2	3.20	3.33	5.12	5.33
3	4.33	2.32	6.65	3.56
4	8.32	8.02	11.39	10.98
5	17.76	1.52	25.84	2.21
6	1.04	1.71	1.57	2.58
7	0.50	0.76	0.74	1.13
8	0.33	0.09	0.49	0.13
9	7.07	1.24	9.58	1.68
10	5.16	4.72	7.41	6.77
Mean	5.04	2.60	7.30	3.80

Table 6. Differential values and error rates of participant B (light skin color)

Item / Iteration	Green Raw Trace V.S ECG Differential Value (BPM)	ICA V.S ECG Differential Value (BPM)	Green Raw Trace V.S ECG Error Rate (%)	ICA V.S ECG Error Rate (%)
1	18.10	1.68	28.81	2.67
2	0.86	0.77	1.40	1.24
3	1.27	1.32	2.07	2.15
4	3.45	3.68	5.27	5.62
5	3.10	0.44	5.10	0.72
6	6.21	6.26	9.42	9.49
7	0.45	0.65	0.64	0.92
8	1.39	1.27	2.02	1.84
9	0.92	0.98	1.33	1.42
10	1.17	0.79	1.82	1.23
Mean	3.69	1.78	5.79	2.73

Experimental Results:

Table 7. Differential values and differential value standard deviation of Case 1

Item / Participant	Green Raw Trace V.S ECG Maximum Differential Value (BPM)	Green Raw Trace V.S ECG Differential value standard deviation (BPM)	ICA V.S ECG Maximum Differential Value (BPM)	ICA V.S ECG Differential value standard deviation (BPM)
A	28.60	8.12	6.39	1.98
B	17.76	4.95	8.02	2.19
C	18.10	5.08	6.26	1.73

5.2 Case 2: Comparison Between Before and After Exercise

In Case 2, only one participant was employed. The measurement time for each iteration was 30 s. A total of 20 iterations were conducted; 10 iterations for each test before and after exercise. The physical condition of the participant before exercise was at an average status, whereas the physical condition after exercise was like that after 5 min of aerobic exercise. The purpose of this experiment was to identify whether the heartbeat measurements increased the error rates because of increased heartbeats.

Experimental Data:

Table 8. Data before exercise

Item / Iteration	Green Raw Trace (BPM)	ICA (BPM)	ECG Data (BPM)
1	62.87	62.87	66.88
2	67.23	67.54	67.61
3	64.48	64.54	69.79
4	67.64	67.61	68.06
5	73.40	73.74	70.55
6	68.34	68.41	70.81
7	69.41	69.28	69.16
8	68.17	68.05	68.70
9	20.57	68.46	69.97
10	70.26	70.26	70.53

Table 9. Data after exercise

Item / Iteration	Green Raw Trace (BPM)	ICA (BPM)	ECG Data (BPM)
1	82.02	128.68	131.45
2	101.58	100.40	102.88
3	98.49	98.44	105.41
4	100.14	99.91	99.30
5	97.44	98.97	100.91
6	97.72	96.53	97.63
7	56.20	86.92	89.97
8	85.61	86.42	88.27
9	84.74	83.28	86.31
10	81.43	82.03	89.10

Error Rate Comparison:

Table 10. Differential values and error rates before exercise

Item / Iteration	Green Raw Trace V.S ECG Differential Value(BPM)	ICA V.S ECG Differential Value(BPM)	Green Raw Trace V.S ECG Error Rate (%)	ICA V.S ECG Error Rate (%)
1	4.01	4.01	6.00	6.00
2	0.38	0.07	0.56	0.10
3	5.31	5.25	7.61	7.52
4	0.42	0.45	0.62	0.66
5	2.85	3.19	4.04	4.52
6	2.47	2.40	3.49	3.39
7	0.25	0.12	0.36	0.17
8	0.53	0.65	0.77	0.95
9	49.40	1.51	70.60	2.16
10	0.27	0.27	0.38	0.38
Mean	**6.59**	**1.79**	**9.44**	**2.59**

Table 11. Differential values and error rates after exercise

Item / Iteration	Green Raw Trace V.S ECG Differential Value (BPM)	ICA V.S ECG Differential Value (BPM)	Green Raw Trace V.S ECG Error Rate (%)	ICA V.S ECG Error Rate (%)
1	49.43	2.77	37.60	2.11
2	1.30	2.48	1.26	2.41
3	6.92	6.97	6.56	6.61
4	0.84	0.61	0.85	0.61
5	3.47	1.94	3.44	1.92
6	0.09	1.10	0.09	1.13
7	33.77	3.05	37.53	3.39
8	2.66	1.85	3.01	2.10
9	1.57	3.03	1.82	3.51
10	7.67	7.07	8.61	7.93
Mean	**10.77**	**3.09**	**10.08**	**3.17**

Experimental Results:

Table 12. shows that accelerated heartbeats did not substantially affect the measurement results.

Table 12. Differential values and differential value standard deviation of Case 2

Item / Exercise	Green Raw Trace V.S ECG Maximal Differential Value (BPM)	Green Raw Trace V.S ECG Differential Value Standard Deviation (BPM)	ICA V.S ECG Maximal Differential Value (BPM)	ICA V.S ECG Differential Value Standard Deviation (BPM)
Before	**49.40**	**14.37**	**5.25**	**1.75**
After	**48.98**	**15.98**	**2.56**	**2.11**

5.3 Case 3: Comparison of Different Measurement Times

In Case 3, three measurement times, which were 20 s, 10 s, and 5 s, were divided for a single participant. The participant's physical condition was at an average status. The purpose of the experiment was to measure whether different times affect error rates. The measurement for 30 s was conducted in Cases 1 and 2; thus, no additional test was conducted.

Experimental Data:

Table 13. Data for a measurement time of 20 s

Item / Iteration	Green Raw Trace (BPM)	ICA (BPM)	ECG Data (BPM)
1	59.26	65.54	68.22
2	54.11	53.47	58.81
3	57.75	56.60	57.13
4	59.79	60.55	58.23
5	57.05	56.55	59.00
6	54.91	60.61	60.04
7	56.99	65.28	64.20
8	61.68	60.49	62.09
9	60.40	62.13	62.20
10	61.16	62.50	62.40

Table14. Data for a measurement time of 10 s

Item / Iteration	Green Raw Trace (BPM)	ICA (BPM)	ECG Data (BPM)
1	58.53	71.43	67.30
2	57.70	59.58	61.18
3	57.99	58.23	60.45
4	86.97	52.60	58.45
5	57.73	59.58	61.00
6	41.62	59.56	60.09
7	61.11	60.55	59.09
8	59.15	59.64	62.20
9	60.93	64.82	61.09
10	58.18	59.44	58.36

Table 15. Data for a measurement time of 5 s

Item / Iteration	Green Raw Trace (BPM)	ICA (BPM)	ECG Data (BPM)
1	54.52	59.77	63.00
2	57.96	120.12	67.14
3	20.40	60.06	58.71
4	56.33	59.83	59.00
5	57.36	60.06	57.71
6	56.88	60.29	57.75
7	47.66	59.94	59.14
8	60.81	60.12	58.71
9	61.15	60.00	61.14
10	38.23	59.24	62.76

Error Rate Comparison:

Table 16. Differential values and error rates for a measurement time of 20 s

Item / Iteration	Green Raw Trace V.S ECG Differential Value (BPM)	ICA V.S ECG Differential Value (BPM)	Green Raw Trace V.S ECG Error Rate (%)	ICA V.S ECG Error Rate (%)
1	8.96	2.68	13.13	3.93
2	4.70	5.35	7.99	9.09
3	0.62	0.53	1.09	0.92
4	1.56	2.32	2.68	3.98
5	1.95	2.45	3.31	4.16
6	5.13	0.57	8.54	0.94
7	7.21	1.08	11.23	1.69
8	0.41	1.60	0.67	2.58
9	1.80	0.07	2.89	0.11
10	1.24	0.10	1.98	0.16
Mean	3.36	1.67	5.35	2.76

6 Conclusion

This study proposes a set of image-based noncontact heartbeat measurement methods that involve using varying human face absorptions of light to detect heartbeats. By performing image processing and ICA, the hidden information in images were identified and concentrated. Subsequently, the frequency domain transformation and heartbeat estimation processes were used for achieving noncontact automatic measurement. By applying Cases 1-3 and after a total of 80 iterations of measurements, using ECG measurement values as the indicators, a differential value percentage higher than 5% was identified as an error measurement [19]. The results are presented in Table 17.

Table 17. Measurement of error rates

Method \ Item	Number of items with a percentage of differential values higher than 5%	Error rate (%)
Green trace	33	41.25
ICA	18	22.5

Table 17 indicates that, regarding the measurement error rates, the ICA processing reduced error rates by 19%, improving the original values measured using green light variations only. In the three cases of this study, the results clearly indicate that skin color and heartbeat rates do not affect measurements. Moreover, at a video camera sampling rate of 30 FPS, one iteration of heartbeat measurement can be completed in 10 s.

In the future, programs will be able to be integrated with human face recognition to reduce environmental factors and enable the popularization of the proposed measurement technology among average households and individuals. This measurement method can be integrated into any device that displays human faces, such as a mirror in a family home. For individual uses, smartphone applications can be created to enable the users to monitor their physiological information while driving or in any other situations anytime.

Acknowledgements

This paper is supported by research project of Ningde Normal University : Real-Time Measurement and Reasearch of Physiological Information (Project No.: JK2015053) and Device-to-device (D2D) Communication Technology and Application (Project No.: JZ160487). And TamKang University: Ministry of Science and Technology, Republic of China, under grant MOST 106-2221-E-032-003-.

References

[1] K.-L. Hsieh, An implementation of individual ECG acquisition system, [master's thesis] New Taipei, Taiwan: Tamkang University, 2006.

[2] Y.-H. Chen, A study on the correlation among, heart rate, PPG, and non-invasive pulse signals, [master's thesis] Taichung, Taiwan: Feng Chia University, 2005.

[3] F.-H. Lien, The design of a non-contact vital-sign sensor, [master's thesis] Taipei, Taiwan: National Taipei University of Technology, 2013.

[4] L. Kong, Y. Zhao, L. Dong, Y. Jian, X. Jin, B. Li, Y. Feng, M. Liu, X.-H. Liu, H. Wu, Non-contact detection of oxygen saturation based on visible light imaging device using ambient light, Optics Express 21(15)(2013) 17464-17471.

[5] D.J. Mordant, I. Al-Abboud, G. Muyo, A. Gorman, A. Sallam, P. Ritchie, A.R. Harvey, A.I. McNaught, Spectral imaging of the retina, Eye 25(3)(2011) 309-320.

[6] T.W. Lee, Independent Component Analysis: Theory and Applications, Kluwer Academic Publishers, Boston, MA, 1998.

[7] W. Verkruysse, L.O. Svaasand, J.S. Nelson, Remote plethysmographic imaging using ambient light, Optics Express 16(26)(2008) 21434-21445.

[8] C. Jutten, J. Herault, Blind separation of Independent sources, part I: an adaptive algorithm based on neuromimetic architecture, Signal Processing 24(1991) 1-10.

[9] P. Comon, Independent component analysis, A new concept?, Signal Processing, Elsevier 36(1994) 287-314.

[10] A. Hyvarinen, A family of fixed-point algorithms for independent component analysis, in: Proc. IEEE International Conference on Acoustics, Speech, and Signal Processing, 1997.

[11] T.-W. Lee, A. Ziehe, R. Orglmeister, T.J. Sejnowski, Combining time-delayed decorrelation and ICA: toward solving the

cocktail party problem, in: Proc. IEEE International Conference on Acoustics, Speech and Signal Processing, 1998.

[12] A. Hyvärinen, J. Karhunen, E. Oja, Independent Component Analysis, vols. 46, John Wiley & Sons, New York, 2001.

[13] A. Hyvärinen, E. Oja, Independent component analysis: algorithms and applications, Neural Networks 13(2000) 411-430.

[14] A. Hyvärinen, New approximations of differential entropy for independent component analysis and projection pursuit, in: Proc. Advances in Neural Information Processing Systems, 1998.

[15] T. Pursche, J. Krajewski, R. Moeller, Video-based heart rate measurement from human faces, in: Proc. IEEE International Conference On Consumer Electronics, 2012.

[16] M. Lewandowska, J. Ruminski, T. Kocejko, J. Nowak, Measuring pulse rate with a webcam-a non-contact method for evaluating cardiac activity, in: Proc. Federated Conference on Computer Science and Information Systems, 2011.

[17] M. Garbey, N. Sun, A. Merla, I. Pavlidis, Contact-free measurement of cardiac pulse based on the analysis of thermal imagery, IEEE Transactions on Biomedical Engineering 54(8)(2007) 1418-1426.

[18] M.Z. Poh, D.J. McDuff, R.W. Picard, Advancements in noncontact, multiparameter physiological measurements using a webcam, IEEE Transactions on Biomedical Engineering 58(1)(2010) 7-11.

[19] C.-L. Wang, W.-J. Chen, W.-J. Ho, L.-A. Hsu, N.-J. Cheng, T.-S. Hsu, C.-T. Kuo, Assessment of doppler-derived aortic flow in atrial fibrillation using beats with equal subsequent cycles, Acta Cardiologica Sinica 22(1)(2006) 16-23.